J. Inst. Eng. India Ser. C (June 2018) 99(3):329–337
https://doi.org/10.1007/s40032-017-0385-7

ORIGINAL CONTRIBUTION

Numerical Investigation of Aerodynamic Braking for a Ground Vehicle

Jaya Krishna Devanuri[1]

Received: 29 July 2015 / Accepted: 1 September 2017 / Published online: 4 October 2017

Abstract The purpose of this article is to observe the effect of an air brake on the aerodynamics of a ground vehicle and also to study the influence of change in the parameters like the velocity of the vehicle, the angle of inclination, height, and position of the air brake on the aerodynamics of the vehicle body. The test subject used is an Ahmed body which is a generic 3D car body as it retains all the aerodynamic characteristics of a ground vehicle. Numerical investigation has been carried out by RNG k-ε turbulence model. Results are presented in terms of streamlines and drag coefficient to understand the influence of pertinent parameters on flow physics. It is found that with the use of an air brake, though the drag coefficient remains more or less constant with velocity, it increases with the increase in height and angle of inclination of the air brake. But the effect of position of air brake on the coefficient of drag is surprising since for certain heights of the air brake the drag coefficient is maximum at the foremost point and as the air brake moves towards the rear it is first observed to decrease and then increase. It is also observed that with the increase in height of the air brake the drag coefficient monotonically decreases as the position of the air brake is moved towards the rear. Taguchi method has been employed with L16 orthogonal array to obtain the optimal configuration for the air brake. For each of the selected parameters, four different levels have been chosen to obtain the maximum drag coefficient value. The study could provide an invaluable database for the optimal design of an airbrake for a ground vehicle.

Keywords Aerodynamics · Computational fluid dynamics · Aerodynamic brake · Ahmed body · Ground vehicle · Optimization · Taguchi method

Abbreviations

ABS	Anti-lock braking system
BL	Boundary layer
RNG	Re-normalization group

Notations

Adj MS	Adjusted mean squares
Adj SS	Adjusted sums of squares
C_D	Drag coefficient
$C_{1\varepsilon}$, $C_{2\varepsilon}$, C_μ, σ_ε, σ_k	RNG k-ε model parameters
DF	Total degrees of freedom
F	F-value
G	Gravity, 9.81 m/s^2
H	Height of the air brake, cm
K	Turbulent kinetic energy per unit mass, m^2/s^2
L	Length of the car, m
P	Pressure, N/m^2
p	p value
Re	Reynolds number
Seq SS	Sequential sums of squares
S_{ij}	Mean strain rate tensor
U	Velocity, m/s
V	Velocity of the vehicle, m/s
X	Length of the air brake from the defined origin, cm

✉ Jaya Krishna Devanuri
djayakrishna.iitm@gmail.com

[1] Department of Mechanical Engineering, National Institute of Technology Warangal, Warangal 506004, Telangana State, India

Greek letters

ρ	Density, kg/m^3
μ	Viscosity, N-s/m^2
ε	Dissipation rate of turbulent kinetic energy per unit mass, m^2/s^2
θ	Angle of Inclination of the air brake, degree
σ_ε,σ_k	Constants in RNG k-ε model
η	Ratio of turbulence to mean shear time scale
η_o	RNG k-ε model parameter

Subscripts

Eff	Effective
i, j, k	Spatial coordinates
t	Turbulent

Introduction

Braking system is one of the most crucial part of any automobile. The conventional braking, that is, mechanical braking is ubiquitous in the automotive world. The conventional braking is achieved due to friction between a stationary part when acted against a rotating part [1]. With the evolution of high speed cars or colloquially called fast cars, braking systems also had to improve. Hence came in innovations like disc brakes, ceramic discs, ABS [2]. But simultaneously, though gradually, aerodynamic brake or 'air brake' was also developed by getting inspired from their airplane counterparts. Though these kinds of air brakes are exclusive to fast moving cars, the principle is to increase the drag force acting on the automobile [3]. It may be noted that at low speeds the aerodynamic brakes are of hardly any use. But the drag forces really become significant as the speed reaches about 45–50 m/s [4]. History tells us that one of the first attempts at using such an air brake was in the Mercedes 300 SLR in 1955 in the Le Mans 24 Hour Challenge and was driven by the racing legend Fangio [5]. Cars like the Bugatti Veyron also use a rear air brake wherein the rear wing itself acts as an air brake [6]. It was observed that in most of the passenger cars, the boundary layer separates just behind the car thus creating a wake behind the car. The resultant pressure drag accounts for about 85% of the total drag on the car [7]. A larger wake implies more drag [8]. The principle behind the air brake is to prepone the separation of the boundary layer thus increasing the size of the wake. Further the air brake also increases the net effective frontal area which also adds to the net increase in the drag force, albeit not as significantly as the increase in the drag coefficient. A detailed numerical analysis of a ground vehicle with an air brake can provide an insight of flow physics and can enhance the understanding of phenomena of drag on the vehicle. Therefore, in the present study the influence of air brake on the drag coefficient is quantitatively examined. Since of all the regular shapes, a flat plate will offer the highest drag coefficient [8], it is logical to use the same as an air brake. It may be noted that any further reference to the air brake in the article would mean a flat plate.

Further, the study provides an insight of flow physics and variation of drag coefficient with parameters like angle of inclination, the brake's height, the position of the brake and speed. To analyze the proposed parameters, an Ahmed body [7] is used as the test subject. Emmanuel [9] considered the Ahmed body to study the influence of flow structure on the drag. It was mentioned that the insight of the flow behavior can be better understood by considering a simplified vehicle shape as employed by Ahmed, et al [7] in spite of going for a real life automobile due to its very complex shape. As Ahmed body generates similar flow structures and near wake as that of a real ground vehicle Ahmed body may be considered over a real automobile. Bruneau, et al [10] have used a square back Ahmed body to study different active and passive control techniques to reduce the drag coefficient. Hsu and Davis [11] considered a 3D Ahmed baseline model to investigate new add on devices to reduce drag of a tractor trailer. It was mentioned that the predicted drag coefficient could satisfactorily agree with experimental data. It may be noted that Ahmed body has been used as a reference body to observe the effects of using aerodynamic devices like vortex generators [12] and rear diffusers [13]. Therefore, by considering the above literature Ahmed body has been considered as the test subject to study the influence of change in the parameters like the velocity of the vehicle, the angle of inclination, height, and position of the air brake on the aerodynamics of the vehicle body.

Along with the understanding of individual parameters on drag coefficient the optimized set of values will be very much needed for the efficient design of an air brake. Taguchi method can be considered as a powerful tool to study the influence of various parameters based on orthogonal array. The method provides an optimum set of parameters with minimum variance [14]. Taguchi-analysis of variance (ANOVA) method can be employed to minimize the number of simulation runs using an orthogonal array. Follett, et al. [15] used Taguchi method to optimize different nozzle configurations for bell annular tri-propellant engine. Juan and Piniella [16] employed CFD-Taguchi method to study the flow over four digit NACA airfoil using signal to noise (S/N) ratio concept. Jafari, et al. [17] used CFD- Taguchi method to study the influence of controllable parameters on thermo-magnetic convection in Ferro-fluids. Jaya and Ruturaj [18] developed a correlation by using CFD-Taguchi-regression analysis. Based on the above literature it may be noted that Taguchi-ANOVA can be an attractive option to obtain the optimum set of

parameters for the design of an air brake with maximum drag coefficient. Therefore, in the present study initially the influence of pertinent parameters, namely, velocity of the vehicle, the angle of inclination, height, and position of the air brake on the drag coefficient is studied. Later, by employing an orthogonal array of Taguchi, the S/N ratio of each simulation is evaluated and the optimal set of parameters are derived.

Numerical Methodology

Test Model

The test model considered in the present study is Ahmed body. Ahmed body is a three-dimensional ground vehicle which retains all the important aerodynamic features of a car. Figure 1 shows the dimensions of an Ahmed body. As the study aims to understand the influence of air brake on the drag of the ground vehicle the Ahmed body is provided with air brake as shown in Fig. 2. The width of the air brake considered is 389 mm. The Reynolds number for flow over a ground vehicle is defined in terms as $Re = \rho VL/\mu$ where L is the length of the vehicle and V is the velocity [7]. The range of Reynolds number considered is 2.6×10^6 (40 m/s) − 4.23×10^6 (60 m/s) which is based on the range of average speed of race cars. A commercial finite volume based tool, Ansys-Fluent is employed for our simulations. The flow field is based on RNG k-ε model derived using the renormalization group theory. The criteria for the selection of RNG k-ε has been discussed in detail and may be referred to Ozalp and Jaya Krishna [19] and Jaya Krishna and Ozalp [20]. The steady state equations [Eqs. (1)–(4)] pertaining to the present study are as follows.

Governing Equations

Continuity equation

$$\frac{\partial(\rho u_i)}{\partial x_i} = 0 \tag{1}$$

Momentum equation

$$\frac{\partial(\rho\, u_i u_j)}{\partial x_j} = \frac{\partial P_{eff}}{\partial x_i} + \frac{\partial}{\partial x_j}\left[\mu_{eff}\left(\frac{\partial u_i}{\partial x_j} + \frac{\partial u_j}{\partial x_i}\right)\right] - \rho g_i \tag{2}$$

k-equation

$$\frac{\partial(\rho\, k\, u_i)}{\partial x_i} = \frac{\partial}{\partial x_j}\left(\left(\mu + \frac{\mu_t}{\sigma_k}\right)\frac{\partial k}{\partial x_j}\right) + G_k - \rho\varepsilon \tag{3}$$

ε-equation

$$\frac{\partial(\rho\, \varepsilon\, u_i)}{\partial x_i} = \frac{\partial}{\partial x_j}\left(\left(\mu + \frac{\mu_t}{\sigma_\varepsilon}\right)\frac{\partial \varepsilon}{\partial x_j}\right) + C_{1\varepsilon}\frac{\varepsilon}{kG_k} - C_{2\varepsilon}\rho\frac{\varepsilon^2}{k} - R_\varepsilon \tag{4}$$

where

$$\mu_{eff} = \mu + \mu_t$$

$$\mu_t = \rho\, C_\mu \frac{k^2}{\varepsilon}$$

$$P_{eff} = P + \frac{2}{3}\rho k$$

$$C_\mu = 0.0845$$

$$C_{1\varepsilon} = 1.42$$

$$C_{2\varepsilon} = 1.68$$

$$C_{3\varepsilon} = \tanh\left|\frac{u_3}{\sqrt{u_1^2 + u_2^2}}\right|$$

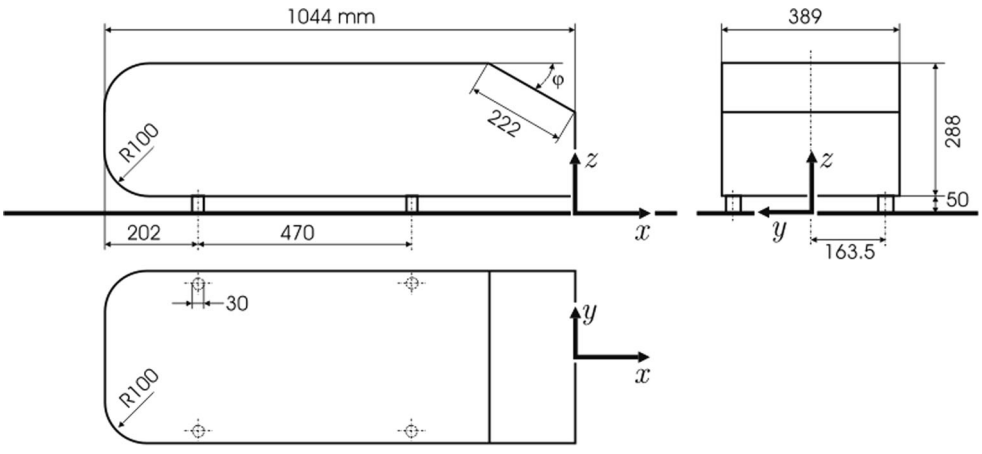

Fig. 1 Side, rear and top views of an Ahmed body

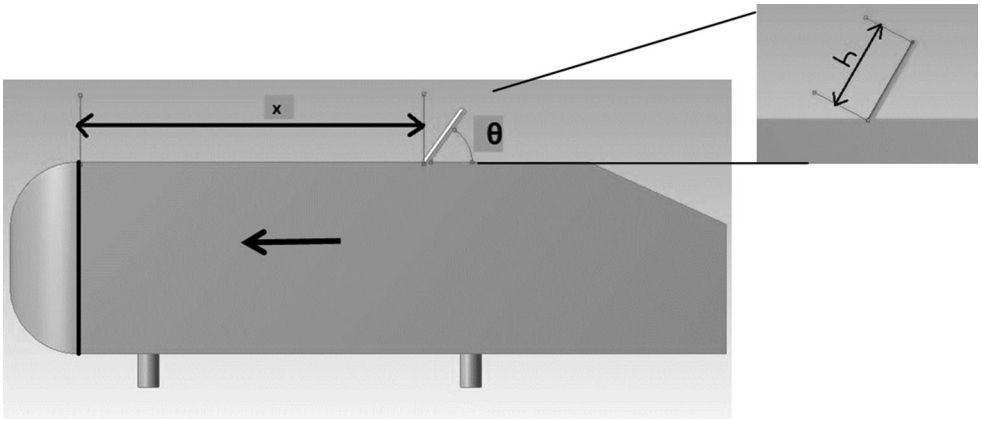

Fig. 2 Position of air brake on Ahmed body

$$G_k = \mu_t S_{ij} \frac{\partial u_i}{\partial x_j}$$

$$R_\varepsilon = \frac{C_\mu \rho \eta^3 (1 - \eta/\eta o)}{1 + \beta \eta^3} \frac{\varepsilon^2}{k}$$

$$\eta = \frac{Sk}{\varepsilon}, \; S = \left(2 S_{ij} S_{ij}\right)^{1/2}, \; \eta_o = 4.38, \; \beta = 0.012$$

$$S_{ij} = \frac{\left(\frac{\partial u_i}{\partial x_j} + \frac{\partial u_j}{\partial x_{\{i}}\right)}{2}$$

$$\sigma_k = 0.7179, \; \sigma_\varepsilon = 0.7179$$

Computational Domain

Since, the Ahmed Body is symmetric about the center plane, only half a model was used for simulation in order to reduce the computational time. The distance between the inlet and the Ahmed Body is five car lengths where one car length is 1044 mm and the distance between the outlet and the Ahmed body is 7.5 car lengths. From both the top and side wall it is at a distance of three car lengths. The lengths have been chosen in order to prevent the wall effects from affecting the solution. No-slip condition was applied to the Ahmed Body and the road. Zero-shear was applied to the top and side walls.

Grid Independence and Validation

Figure 3 shows the mesh for the Ahmed body without the air brake (Fig. 3a) and with air brake (Fig. 3b). The area in the vicinity of the body is provided with a finer mesh in order to capture the wake and boundary effects more efficiently.

It may be noted that the range of Reynolds number considered is 2.6×10^6 (40 m/s) − 4.23×10^6 (60 m/s). Initially the grid independence test was carried out on the Ahmed body without the air brake at a velocity of 60 m/s. It is observed that the variation of drag coefficient between grid sizes of 1,869,075 elements and 2,076,126 elements is observed to be less than 1%. Therefore a grid size of 1,869,075 elements has been considered. The value of drag coefficient thus obtained for 60 m/s is 0.281 which is in good agreement with the experimental value of 0.28 [21].

In line to the earlier, the grid independence test has been performed for the Ahmed body with air brake. The variation of drag coefficient values for a velocity of 60 m/s between 1,974,608 and 2,328,103 elements is observed to be less than 1%. Therefore an element size of 1,974,608 has been considered for the parametric study.

Simulation Details for Optimization

Four parameters, namely, velocity of the vehicle (V), height (h), inclination (θ) and position (x) of the air brake each with four levels within the operating range of the input parameters ($40 \leq$ V, m/s ≤ 60, $5 \leq$ h, cm ≤ 20, $15 \leq \theta$, degree ≤ 75 and $0 \leq$ x, cm ≤ 50) have been considered. By employing Taguchi method an L16 orthogonal array with 16 different simulations at four levels are studied. The details pertaining to input parameters with their values considered at each level used for orthogonal array is provided in Table 1.

Results and Discussion

The aim of the present study is to understand the flow physics of the air brake and its pertinent parameters on the drag of the Ahmed body. Therefore the study is classified into three parts. In the first part, the effect of the use of the air brake on the drag coefficient is studied and is followed by the results of the parametric studies in the second part. The parameters considered are angle of inclination of the air brake (θ), position of the air brake (x) and height (h) of the brake plate which are as shown in Fig. 2. In the third part the optimum set of parameters for the drag coefficient

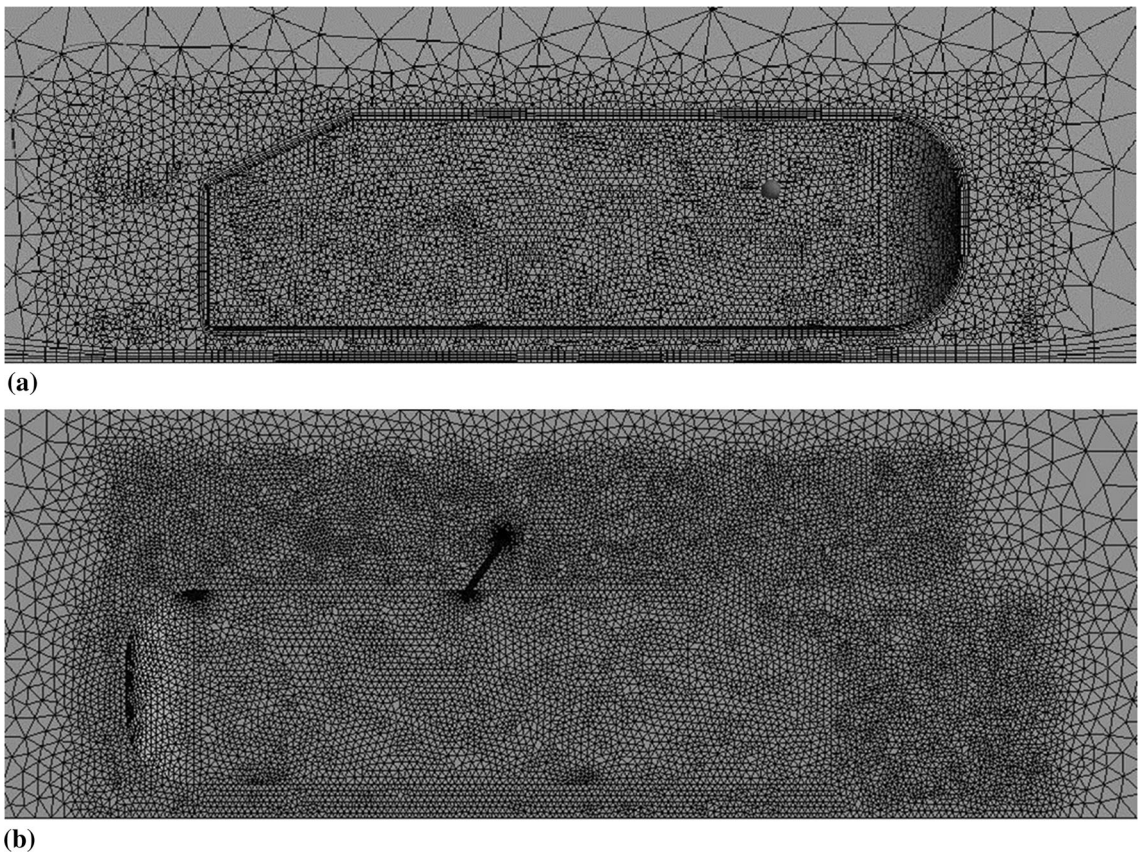

Fig. 3 Mesh **a** without air brake **b** with air brake

Table 1 Input parameters and level values for L16 orthogonal array

Input parameters	Levels			
	1	2	3	4
Velocity, V, m/s	40	50	55	60
Height, h, cm	5	10	15	20
Inclination of air brake, θ, degree	15	35	55	75
Position, x, cm	0	15	35	50

is obtained by employing Taguchi method with L16 orthogonal array.

Effect of Air Brake

In order to study the influence of air brake the comparison is made for the vehicle with and without air brake. The position of air brake is as shown in the Fig. 2. In this case the angle of inclination of the air brake is taken as $\theta = 55°$ its position is $x = 0$ and height $h = 7$ cm with a vehicle's velocity of 40 m/s ($Re = 2.6 \times 10^6$). The streamlines thus obtained without and with air brake are shown in Fig. 4. It is observed that with the presence of air brake the drag coefficient has increased from 0.28 (without air brake) to 0.44 (with air brake) which represents an increase of 57.2%. The reason can be attributed to the early separation of the boundary layer thus creating a larger wake and hence more drag as can be seen from Fig. 4.

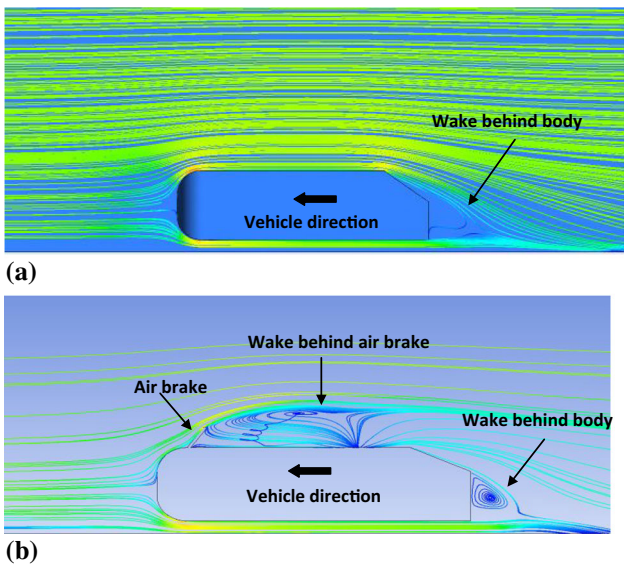

Fig. 4 Streamlines for flow over the vehicle **a** without air brake **b** with air brake

Effect of Change in Parameters

Variation with Velocity of the Vehicle (V)

To study the influence of vehicle speed the parameters such as position, inclination and height of the air brake are kept constant and the velocity is varied from 40 m/s to 60 m/s with every 5 m/s increment in the velocity. The air brake is fixed at a position, x = 0 cm, the angle of inclination, θ = 55° and the height of the brake, h = 10 cm. The results thus obtained for the variation of drag with the velocity of the vehicle are provided in Table 2. For the considered range of velocity the flow pattern is observed to follow a similar trend as shown in Fig. 4b. A recirculation zone is observed behind the air brake and also at the trailing portion of the vehicle.

From Table 2 it may be inferred that the influence of vehicle's velocity for the considered range is insignificant. It may be noted that the variation of drag coefficient of the vehicle with velocity is similar to the variation observed for the drag coefficient of the Ahmed body without the air brake [7]. Further, similar trend can be expected for the variation of drag coefficient with speed due to the change in other parameters. Hence, the velocity of the vehicle can be considered as 40 m/s in the subsequent parametric studies.

Variation with Angle of Inclination (θ)

The details pertaining to angle of inclination (θ) may be referred to Fig. 2. In order to understand the influence of the angle of inclination, θ is varied from 15° to 75° by fixing other parameters, that is, position (x) = 50 cm, height (h) = 10 cm and velocity (V) = 40 m/s. The trend pertaining to the variation of drag coefficient with the angle of inclination is provided in Table 3. As expected with the increase of 'θ' the value of drag coefficient increased monotonically. The increase is due to the fact that as the angle of inclination is increased, the amount of wake formed behind the brake also increased leading to an increase in drag coefficient of the vehicle.

Variation with Height (h)

The variation of drag coefficient with height for the air brake when position x = 50 cm, angle of inclination θ = 55° and velocity V = 40 m/s is given in Table 4. The details pertaining to variation in height (h) of the air brake may be referred to Fig. 2. It may be noted that the maximum limit on the brake height is set by the possibility of mechanical failure of the brake due to bending moment being higher the critical value. It can be observed that with the increase in height of the air brake drag coefficient is observed to increase monotonically. The primary reason is due to the increase in size of the wake behind the air brake with the increase in the air brake's height.

Variation with Position (x)

To study the influence of the position of the air brake the velocity is set at 40 m/s, the height of the air brake is taken

Table 2 Variation of drag coefficient with velocity of the vehicle

Velocity of the vehicle, V, m/s	Drag coefficient, C_D
40	0.42
45	0.42
50	0.42
55	0.43
60	0.44

Table 3 Variation of drag coefficient with angle of inclination

Angle of inclination, θ, degree	Drag coefficient, C_D
15	0.29
55	0.38
60	0.41
75	0.44

Table 4 Variation of drag coefficient with height of the brake

Height of the brake, h, cm	Drag coefficient, C_D
7	0.42
10	0.44
15	0.49
20	0.52

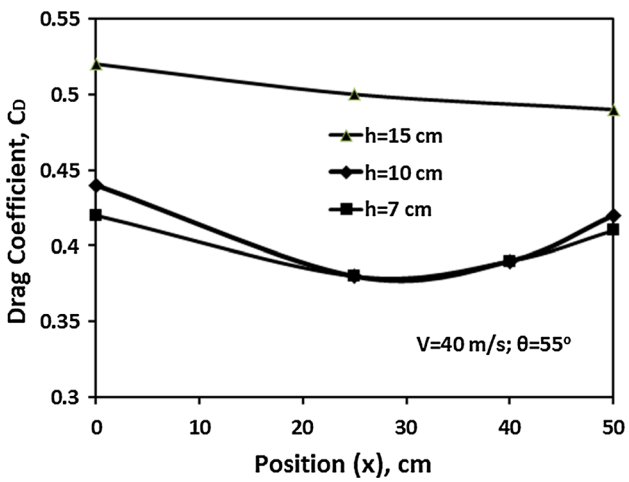

Fig. 5 Variation of drag coefficient with position

at h = 10 cm and inclination at θ = 55°. The parameter 'x' is used to define the position as shown in Fig. 2. The variation of drag coefficient with the position of the air brake is observed by varying 'x' from 0 to 50 cm. The trend for the variation of drag coefficient with the position of air brake for h = 10 cm is given in Fig. 5. It is expected that as the air brake is moved towards the rear, the recirculation zones at the back portion of the air brake and a rear slant portion of the vehicle may boil down to a smaller wake at the rear portion which may lead to decrease in drag coefficient. But surprisingly results suggest a decrease and then increase in the drag coefficient. In the case of the Ahmed body as shown in Fig. 4a without the air brake, the separation occurs at the rear slant portion of the vehicle.

To understand the flow physics of the phenomenon provided in Fig. 5, streamlines are plotted over the vehicle with the air brake of height (h) = 10 cm placed at x = 40 cm and x = 50 cm and are shown in Fig. 6. As shown in Fig. 6a with the air brake at the position x = 40 cm, there is a wake formation behind the air brake and a possible hint of reattachment of flow and a second separation at the rear of the vehicle. But in the case of the brake been placed at x = 50 cm as seen in Fig. 6b, there is a separation behind the air brake. But the area around the vehicle's rear portion falls in the wake of this initial separation and thus altogether a larger wake is formed. The increase in size of the wake for x = 50 cm when compared to that of x = 40 cm contribute to the increase in drag coefficient. From Fig. 5 it may be noted that for x = 0 the drag coefficient is higher to that of x = 40 cm and 50 cm. This behavior can be inferred to the formation of recirculation zones both at the rear portion of the air brake and rear slant portion of the vehicle.

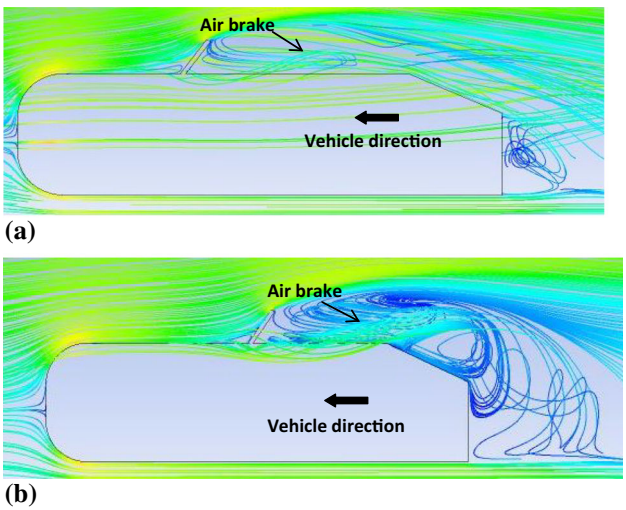

Fig. 6 Streamlines over the vehicle with the air brake placed at **a** x = 40 cm; **b** x = 50 cm

In order to further analyze this unusual behavior, the influence of the position of the air brake with a variation of height (that is, h = 15 and 7 cm) is also studied. When the height of the brake is 15 cm, as shown in Fig. 5 the drag coefficient is observed to decrease with the increase in position from 0 to 50 cm. At x = 0 with h = 15 cm a larger wake preventing the reattachment of flow at the back portion of the air brake and the wake at the rear portion of the vehicle lead to a drag coefficient value of 0.52. When the position of this air brake moves towards the rear, the wake at the back portion of the air brake is observed to gradually reduce resulting in the decrease of drag coefficient. The variation of the drag coefficient for h = 7 cm with position is given in Fig. 5. Similar trend may be observed for h = 7 cm as that of h = 10 cm. The marginal variation at x = 0 is due to the reduction in obstruction to flow area when the height of the air brake (h) is reduced from 10 cm to 7 cm. But when the position is varied from 15 cm to 45 cm for heights 7 cm and 10 cm did not make any difference due to the reattachment of the boundary layer as seen in Fig. 6a.

Optimization of Air Brake Parameters using Taguchi Method

Taguchi method is a promising tool to study the influence of process parameters by using an orthogonal array (OA) to attain optimized economical results [14]. The method accentuates the use of loss function by which the S/N (signal to noise) ratio can be evaluated to obtain an optimal solution. In this study L16 orthogonal array as shown in Table 5

Table 5 L16 orthogonal array

Velocity, V, m/s	Height, h, cm	Inclination, θ, degree	Position, x, cm	Drag coefficient, C_D
40	5	15	0	0.37
40	10	35	15	0.51
40	15	55	35	0.61
40	20	75	50	0.76
50	5	35	35	0.36
50	10	15	50	0.38
50	15	75	0	0.67
50	20	55	15	0.57
55	5	55	50	0.45
55	10	75	35	0.53
55	15	15	15	0.34
55	20	35	0	0.52
60	5	75	15	0.47
60	10	55	0	0.55
60	15	35	50	0.5
60	20	15	35	0.37

Table 6 Response for signal to noise ratios (larger is better)

Level	Velocity, V, m/s	Height, h, cm	Inclination, θ, degree	Position, x, cm
1	−5.29	−7.751	−8.762	−5.747
2	−6.41	−6.24	−6.606	−6.665
3	−6.875	−5.791	−5.326	−6.829
4	−6.602	−5.396	−4.484	−5.936
Delta	1.585	2.355	4.278	1.083
Rank	3	2	1	4

Table 7 ANOVA (analysis of variance) for SN ratios

Source	DF	Seq SS	Adj SS	Adj MS	F	P	Percentage contribution
Velocity	3	5.8123	5.8123	1.9374	41.12	0.006	9.12
Height	3	12.7443	12.7443	4.2481	90.16	0.002	20.00
Inclination	3	41.6026	41.6026	13.8675	294.33	0	65.30
Position	3	3.4072	3.4072	1.1357	24.11	0.013	5.35
Residual	3	0.1413	0.1413	0.0471			0.22
Total	15	63.7077					100.00

is used to perform the simulations. Table 6 show the influence of process parameters on the drag coefficient. The optimum process parameters on the drag coefficient are obtained as velocity at 40 m/s (level 1), height at 20 cm (level 4), inclination at 75° (level 4) and position at 0 cm (level 1). It is seen that higher values of S/N ratio are obtained for lower value of velocity and position, and higher values of height and inclination. The optimised condition to get maximum drag coefficient is for the condition: $V = 40$ m/s, $h = 20$ cm, $\theta = 75°$ and $x = 0$ cm.

The degree of importance of each parameter such as velocity, height, inclination and position is considered for each response and is given in Table 7. From the ANOVA table, it can be observed that that inclination of the air brake is the most significant factor, which affects the drag coefficient with 65.30% contribution while height is the second most significant factor with 20% contribution. As the contribution of velocity and position is less than 10% these parameters can be considered to influence less on drag coefficient when compared to that of inclination and height of the air brake.

Conclusions

The studies conducted in this paper throw light on the parametric analysis of an air brake. The same procedure can be followed to determine the air brake's parameters on any other vehicle. The first objective is to observe the aerodynamic effect of using an air brake. It is followed by parametric analysis and optimization of the air brake on drag coefficient. The following conclusions can be drawn from the present study:

- For the considered velocity range, that is, 40 to 60 m/s the change in drag coefficient of the vehicle with the air brake is more or less negligible.
- As the height of the brake increases the coefficient of drag increases.
- As the angle of inclination of the air brake increases, the coefficient of drag increases.
- The drag coefficient first decreases and then increases as the position of the brake is moved towards the fore of the body for certain heights of the air brake. This effect has been attributed to possible reattachment of flow. A further increase in the height of the brake increases the size of the wake so that there is no reattachment of flow.
- The drag coefficient is highest when the air brake is placed at the foremost point of the Ahmed body. This clearly implies that the use of the air brake would be more effective, at least in terms increase of drag forces if the position of the brake is moved towards the fore of the vehicle as opposed to the current trend of air brakes in which it is placed almost at the rear end of the car.
- Taguchi-ANOVA technique with L16 orthogonal array is employed to attain the optimum set of parameters for the drag coefficient for the considered range of parameters, namely, $40 \leq V$, m/s ≤ 60, $5 \leq h$, cm ≤ 20, $15 \leq \theta$, degree ≤ 75 and $0 \leq x$, cm ≤ 50 for air brake. Based on the study it can be concluded that the optimised condition to attain maximum drag is $V = 40$ m/s, $h = 20$ cm, $\theta = 75°$ and $x = 0$ cm.

The reasons for the above observations are mentioned in their respective sections. It is to be noted that air brakes are not really effective at low speeds. But their effectiveness increases as the velocity of the vehicle increases. As opposed to conventional braking which relies on traction between the tire and the road for its functioning [4], air brakes do not require traction for their working. Hence, air brakes can be crucial in the case of loss of grip between road and tire which occur in phenomena like hydroplaning [22].

Acknowledgements The author is thankful NIT Warangal for assistance in performing simulations.

References

1. P. Ken, *Automobile Braking Systems*, 6th edn. (Cengage Learning, Boston, 2014)
2. W. Jonathan, N. Andrew, D.S. Philip, *The Ultimate History of Fast Cars: Vehicles Built for the Fast Lane* (Parragon Publishing India, Noida, 2011)
3. J. Katz, *Race Car Aerodynamics: Designing for Speed* (Robert Bentley Publishers, Cambridge, 1996)
4. S. Carroll, *Tune to Win* (Aero Publishers, Fall Brook, 1978)
5. L. Trevor, D.S.C. Philip, *The Ultimate History of Mercedes-Benz* (Parragon Pubishing India, Noida, 2010)
6. The Car that Loves to Hold the Road, Popular science magazine. Bon. Corp. **268**(2), 22 (2006)
7. S.R. Ahmed, G. Ramm, G. Faltin, Some salient features of the time-averaged ground vehicle wake. SAE Technical Paper 840300 (1984). doi:10.4271/840300
8. J.D. Anderson-Jr, *Fundamentals of Aerodynamics*, 5th edn. (McGraw Hill, New York, 2014)
9. G. Emmanuel, Computational study of flow around a simplified car body. J Wind Eng. Ind. Aerod. **96**(6–7), 1207–1217 (2008)
10. C.H. Bruneau, C. Emmanuel, D. Delphine, G. Patrick, M. Iraj, Coupling active and passive techniques to control the flow past the square back Ahmed body. Comp. Fluids **39**(10), 1875–1892 (2010)
11. F.H. Hsu, R.L. Davis, New drag reduction design for tractor-trailers using CFD. Int. J. Aerod. **1**(2), 192–205 (2010)
12. G. Pujals, S. Depardon, C. Cossu, Drag reduction of a 3D bluff body using coherent streamwise streaks. Exp. Fluids **49**(5), 1085–1094 (2010)
13. S.K. Das, P. Kumar, S. Rawat, Alterations of formula 3 race car diffuser geometry for optimized downforce. Int. J. Eng. Res. Tech. **6**(3), 351–358 (2013)
14. S. Mukherjee, A. Kamal, K. Kumar, Optimization of material removal rate during turning of SAE 1020 material in CNC lathe using Taguchi technique. Procedia Eng. **97**, 29–35 (2014)
15. W. Follett, A. Ketchum, A. Darian, Y. Hus, Application of optimization techniques to design of unconventional rocket nozzle configurations, *13th Workshop for CFD Applications in Rocket Propulsion Huntsville*, Alabama, 1995, pp. 879–888
16. P. Juan Murcia, A. Pinilla, CFD analysis of blunt trailing edge airfoils obtained with several modification methods. Revista de Ingeniería. **33**, 14–24 (2011)
17. A. Jafari, T. Tynjala, S.M. Mousavi, P. Sarkomaa, CFD Simulation and evaluation of controllable parameters effect on thermomagnetic convection in ferro-fluids using Taguchi technique. J. Comp. Fluids. **37**, 1344–1353 (2008)
18. D.J. Krishna, R.R. Deshpande, Taguchi based methodology to generate correlation via numerical analysis for natural convection in a differentially heated cavity—HMTC1300663, in *Proceedings of the 22nd National and 11th International ISHMT-ASME Heat and Mass Transfer Conference* (IIT Kharagpur, India, 2013)
19. N. Ozalp, D. Jaya Krishna, CFD Analysis on the influence of helical carving in a vortex flow solar reactor. Int. J. Hydrog. Energy **35**(12), 6248–6260 (2010)
20. D. Jaya Krishna, N. Ozalp, Response to the comments made by Khalid M. Saqr on our paper titled-CFD analysis on the influence of helical carving in a vortex flow solar reactor. Int. J. Hydrog. Energy **36**(3), 2323–2326 (2011)
21. I. Bayraktar, D. Landman, O. Baysal, Experimental and computational investigation of Ahmed body for ground vehicle aerodynamics. SAE Technical Paper 2001-01-2742 (2001). doi:10.4271/2001-01-2742
22. R.N. Jazar, *Vehicle Dynamics: Theory and Application* (Springer, New York, 2008)